ACS chemical biology

Articles

pubs.acs.org/acschemicalbiology

Deciphering the Cellular Targets of Bioactive Compounds Using a Chloroalkane Capture Tag

Rachel Friedman Ohana,*[,†] Thomas A. Kirkland,[‡] Carolyn C. Woodroofe,[‡] Sergiy Levin,[‡] H. Tetsuo Uyeda,[‡] Paul Otto,[†] Robin Hurst,[†] Matthew B. Robers,[†] Kris Zimmerman,[†] Lance P. Encell,[†] and Keith V. Wood[†]

[†]Promega Corporation, Madison, Wisconsin, United States

[‡]Promega Biosciences LLC, San Luis Obispo, California, United States

Supporting Information

ABSTRACT: Phenotypic screening of compound libraries is a significant trend in drug discovery, yet success can be hindered by difficulties in identifying the underlying cellular targets. Current approaches rely on tethering bioactive compounds to a capture tag or surface to allow selective enrichment of interacting proteins for subsequent identification by mass spectrometry. Such methods are often constrained by ineffective capture of low affinity and low abundance targets. In addition, these methods are often not compatible with living cells and therefore cannot be used to verify the pharmacological activity of the tethered compounds. We have developed a novel chloroalkane capture tag that minimally affects compound potency in cultured cells, allowing binding interactions with the targets to occur under conditions relevant to the desired cellular phenotype. Subsequent isolation of the interacting targets is achieved through rapid lysis and capture onto immobilized HaloTag protein. Exchanging the chloroalkane tag for a fluorophore, the putative targets identified by mass spectrometry can be verified for direct binding to the compound through resonance energy transfer. Using the interaction between histone deacetylases (HDACs) and the inhibitor, Vorinostat (SAHA), as a model system, we were able to identify and verify all the known HDAC targets of SAHA as well as two previously undescribed targets, ADO and CPPED1. The discovery of ADO as a target may provide mechanistic insight into a reported connection between SAHA and Huntington's disease.

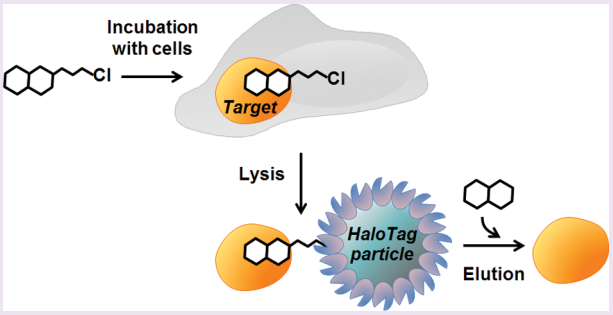

Phenotypic screening of compound libraries is commonly employed as part of the drug discovery workflow.[1,2] This approach monitors the influence of compounds on cellular models reflecting disease biology, thus, providing an opportunity to discover novel compounds with therapeutic potential. However, the utility of phenotypic screening is limited by the challenges associated with identifying the cellular targets eliciting the phenotypic response through interaction with the bioactive compound.[3−6]

Common approaches for target identification rely on affinity enrichment followed by high resolution mass spectrometry.[3,7,8] Traditional enrichment methods utilize a bioactive compound tethered to either a surface or an affinity tag (e.g., biotin) for selective isolation of interacting targets, often from cell lysates.[5,8,9] For these methods to yield meaningful results, it is critical that the chemical modification of the compound does not alter its binding to cellular targets. Unfortunately, verifying this by recapitulating the phenotypic activity is often hindered by the influence of the modification on cell permeability.[3,8,10] Moreover, since drugs frequently bind reversibly to their targets, isolation efficiency depends on a given target's affinity and subsequent dissociation rate. The degree of selectivity of the capture method also affects the ability to detect targets of low abundance over a nonspecific background. Not surprisingly, successful target identification has generally involved high affinity targets expressed at relatively high levels.[5,7−9,11]

Recognizing that the intracellular environment may influence binding between drugs and their targets, methods have been developed allowing modified compounds to engage with their targets inside cells.[9,12,13] These methods typically rely on conjugating the bioactive compound to a small bifunctional tag, comprising a photo-cross-linker for freezing the binding equilibrium and an alkyne or azide for click-chemistry ligation to an affinity tag.[4,12−14] Cross-linking ensures that the binding interactions are preserved over the time required for both chemical ligation and subsequent capture of the affinity tag. However, cross-linking efficiency is often low due to rapid quenching of the reactive group inside cells.[15,16] In addition, nonspecific cross-linking to highly abundant or "sticky" proteins can obscure target detection due to nonspecific background.[6,13,15,16] Furthermore, background can also result from the click reaction, as copper-induced activation of the alkyne group may cause nonspecific protein labeling.[17,18]

Received: May 12, 2015
Accepted: July 10, 2015
Published: July 10, 2015

DOI: 10.1021/acschembio.5b00351
ACS Chem. Biol. 2015, 10, 2316−2324

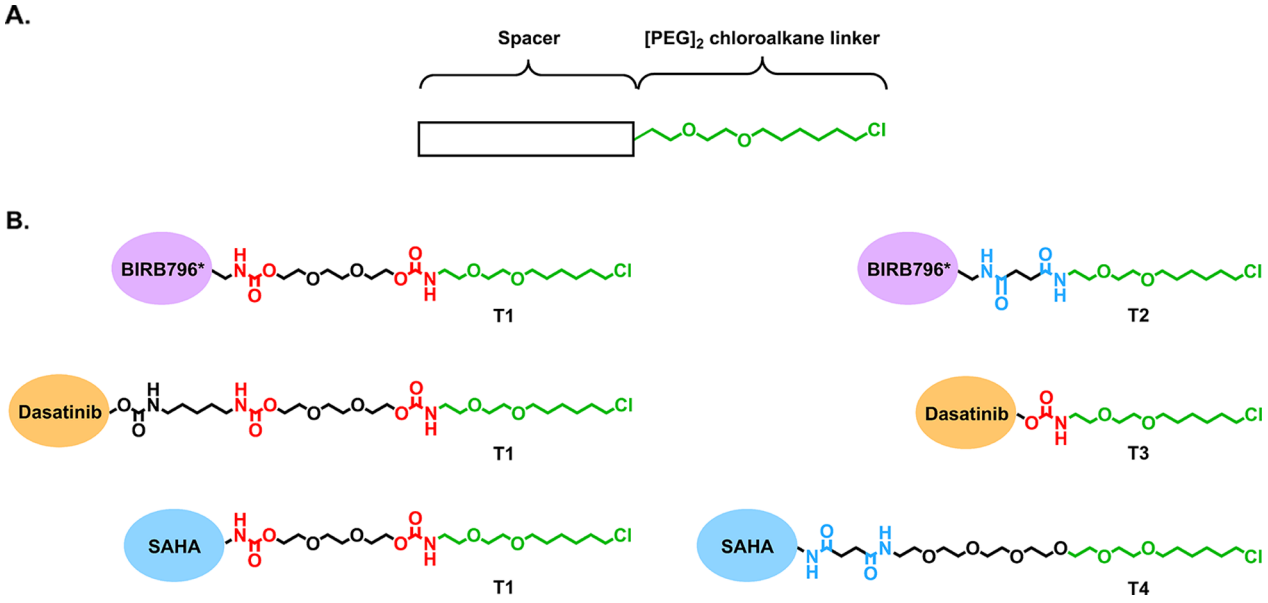

Figure 1. Chemical structures of (A) chloroalkane tag and (B) chloroalkane tags conjugated to different bioactive compounds. The conserved $[PEG]_2$ chloroalkane linker is indicated in green, spacers in black, and amide and carbamate groups in the common spacer structures are indicated in blue and red, respectively.

We developed an alternative approach that does not rely on chemical cross-linking to achieve effective target enrichment from living cells. The method utilizes a novel chloroalkane capture tag that exhibits minimal influence on phenotypic potency when appropriately attached to bioactive compounds. This can be useful for validating the suitability of a tagged compound since proper positioning of the tag is necessary to retain productive binding. As this cannot be demonstrated directly for unknown targets, preservation of pharmacological activity provides a means for confirming retention of relevant binding interactions with cellular targets.

Enrichment of interacting targets is achieved through efficient capture of the chloroalkane tagged compound onto an immobilized HaloTag protein.[19,20] Although cell lysis promotes dissociation of transiently bound targets, this is mitigated by fast sample processing afforded by the rapid binding kinetics of HaloTag.[19,20] The rapid and selective nature of the process also facilitates identification of targets having low affinity or low abundance.

Mass spectrometry analysis of the enriched proteins cannot discriminate between targets able to bind directly to the bioactive compound and proteins that copurify through other mechanisms (e.g., via protein−protein interactions). Ascertaining the true targets and establishing their binding affinities is often a rate limiting step toward understanding the bioactive compound's mechanism of action.[3,7,9] Current approaches to accomplish this include biochemical methods utilizing purified proteins and cellular methods relying on binding-dependent stabilization of targets (e.g., CETSA).[10,21] Instead, we have addressed this using bioluminescence resonance energy transfer (BRET), which provides a sensitive measure of molecular proximity.[22] By exchanging the chloroalkane tag for a suitable fluorophore, direct binding interactions with putative targets genetically fused to NanoLuc luciferase (NLuc)[23] can be verified.[24]

We used Vorinostat (SAHA), an inhibitor of class I and class IIb histone deacetylases (HDACs), as a model compound for investigating the ability of our approach to identify intracellular targets.[25,26] Employing SAHA-chloroalkane to selectively enrich for targets from K-562 cells, we identified and verified all the known HDAC targets of SAHA (i.e., HDAC 1, 2, 3, 6, 8, and 10) and two previously undescribed targets (ADO and CPPED1). One of these novel "off targets," ADO, may provide insight into a reported efficacy for SAHA in the treatment of Huntington's disease.[27]

RESULTS AND DISCUSSION

Design and Development of the Chloroalkane Tag. The value of chloroalkanes as capture tags stems from their relative lack of reactivity in mammalian cells and their ability to bind rapidly and irreversibly to HaloTag.[19,20] We previously reported that a 13-atom chloroalkane linker comprising a $[PEG]_2$ segment (Figure 1, panel A), appended to a TAMRA fluorophore, is cell permeable and efficiently labels HaloTag expressed in mammalian cells.[19,20] We suspected that this linker when conjugated to a bioactive compound may be too short for binding to HaloTag when the compound is also bound to its cellular targets. To increase its length, we inserted additional PEG units to create $[PEG]_4$ and $[PEG]_6$ chloroalkane tags. We also incorporated a carbamate−$[PEG]_3$−carbamate spacer, previously used to attach the chloroalkane linker to a solid support,[20] creating chloroalkane tag T1 (Figure 1, Supporting Information Figure 1). When conjugated to methotrexate and evaluated for binding kinetics to HaloTag, the $[PEG]_4$ and $[PEG]_6$ tags significantly reduced binding kinetics while the longer T1 maintained the rapid binding kinetics of the $[PEG]_2$ linker (Supporting Information Figure 1).

Encouraged by this result, we further examined the length and structure of the spacer by generating chloroalkane tags T2, T3, and T4 (Figure 1, panel B). To minimize bias that could arise from relying on a single bioactive compound, these tags were conjugated to BIRB796 tracer (BIRB796*),[28] dasatinib,[29] and SAHA[25,26] and tested for HaloTag binding, cellular permeability, and target enrichment (Figure 2).

T1, although similar in length to T4 and notably longer than T2, displayed faster binding to HaloTag in cell lysates than both T4 and T2 when appended to SAHA and BIRB796*, respectively. However, when appended to dasatinib and compared to the significantly shorter T3, T1 displayed slower binding to

DOI: 10.1021/acschembio.5b00351
ACS Chem. Biol. 2015, 10, 2316−2324

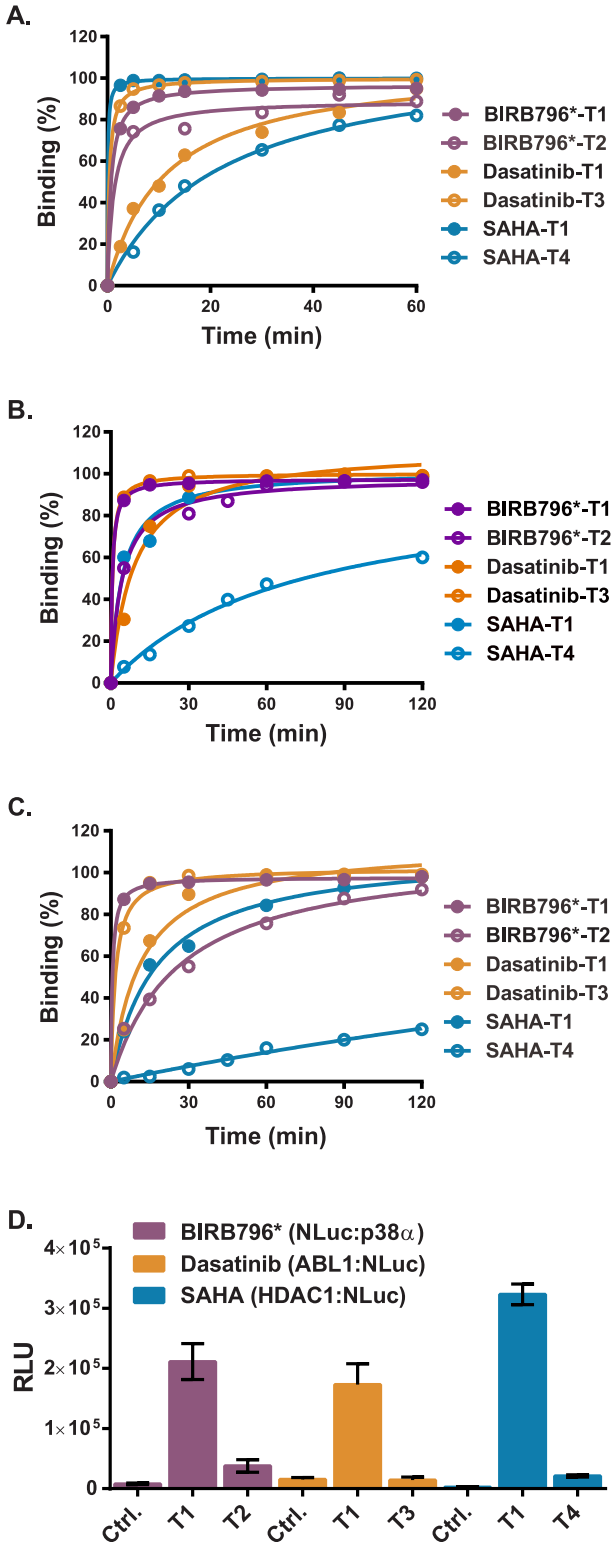

Figure 2. Comparison between the chloroalkane tags for binding kinetics to a HaloTag fusion protein in (A) cell lysate, (B) intact cells (ubiquitous expression), and (C) intact cells (nuclear expression). (D) Specific enrichment of NLuc fusion proteins ($n = 6$). Enrichments using the T1 conjugates were 27-, 11-, and 125-fold over background for BIRB796*, dasatinib, and SAHA, respectively. Significantly less or no enrichment was observed with the other tags.

HaloTag (Figure 2, panel A). These results indicate that T1, despite its length, generally retained good binding kinetics to HaloTag. A docking model of T1 with the crystal structure of HaloTag (PDB 4KAJ) suggests that one of the two carbamates within its structure may form stabilizing hydrogen bonds with two amino acids (Thr148 and Phe144) positioned near the entrance of the HaloTag binding tunnel (Supporting Information Figure 2).

To investigate the ability of these conjugates to permeate cells, they were compared for their binding to HaloTag inside intact cells (Figure 2, panels B and C). A similar kinetic trend was observed for these conjugates, suggesting that membrane permeability is generally not a limiting factor for their binding to HaloTag.

Enrichment efficiency of the chloroalkane conjugates was evaluated using HaloTag immobilized onto paramagnetic particles. Using site-specific chemistry to attach HaloTag through a single point on the N-terminus of the protein, we were able to retain 95% of its specific activity after immobilization (Supporting Information Figure 3). Assessment of relative target enrichment was achieved using known targets of the selected compounds genetically fused to a NLuc reporter.[23] Cells expressing NLuc fusions were incubated with the tagged compounds, while control cells remained untreated. Following cell lysis, the tagged compounds were captured onto HaloTag paramagnetic particles. Interacting targets were then eluted using excess unconjugated compound, and specific enrichment was determined by the increase in bioluminescence over the controls (Figure 2, panel D). T1 provided substantially greater enrichment for all three models. Although T3 displayed fast binding kinetics to HaloTag, it failed to provide significant enrichment, consistent with our presumption that the 13-atom chloroalkane linker alone is too short to allow simultaneous binding to both HaloTag and the target protein. While we did not analyze all possible variations of chloroalkane tags and bioactive compounds, these results taken together indicate that T1 exhibits a suitable combination of good binding kinetics to HaloTag, retention of cellular permeability, and efficient enrichment of target proteins.

Influence of the Chloroalkane Tag on Bioactivity. Ideally, a capture tag should minimally influence the biological activity of compounds introduced to living cells. Since T1 exhibited the highest enrichment efficiency following target engagement inside cells, we further investigated its influence on the potency of BIRB796*, dasatinib, and SAHA (Figure 3). BIRB796* inhibits p38 and JNK kinases, leading to reduced production of pro-inflammatory cytokines such as TNFα.[28,30] In LPS stimulated THP-1 cells, inhibition of TNFα secretion was found to be unaffected by appending T1 onto BIRB796* (Figure 3, panel A). Dasatinib inhibits the BCR-ABL oncogenic signaling pathway, thereby reducing activation of STAT5.[29] Appending T1 onto dasatinib reduced its potency by 3- to 4-fold as determined by repression of STAT5 activation and induction of apoptosis in K-562 cells (Figure 3, panel B). SAHA is a class I/IIb HDAC inhibitor which induces growth arrest and apoptosis of cancer cells.[26] Appending T1 onto SAHA reduced its potency by 3-fold as determined by inhibition of HDAC activity in K-562 cells and activation of apoptosis (Figure 3, panel C). Thus, for these three distinct models, appending T1 had a relatively minor impact on compound potency, suggesting that the tagged compounds retained their ability to permeate cells and engage their expected cellular targets.

Enrichment of Cellular Targets. To evaluate the ability to enrich endogenous targets, we chose SAHA as an experimental model due to several technical challenges it presents. The

DOI: 10.1021/acschembio.5b00351
ACS Chem. Biol. 2015, 10, 2316−2324

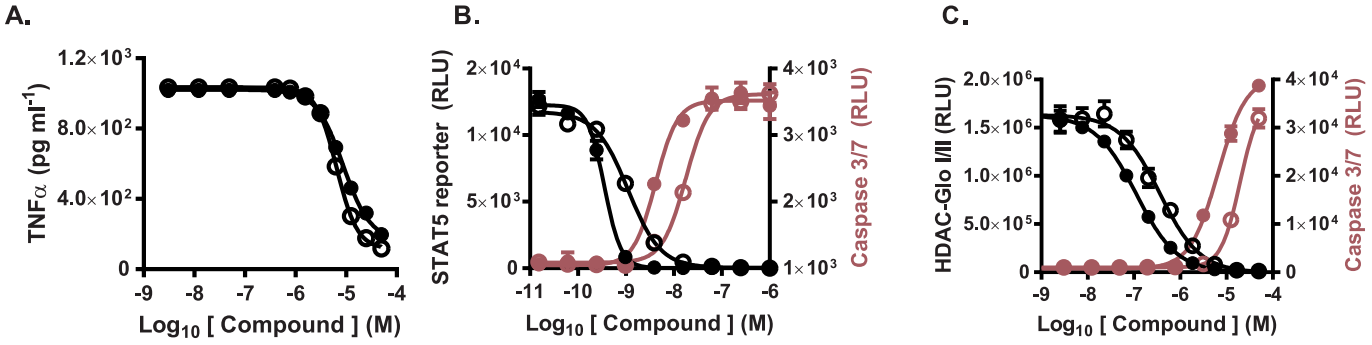

D.

Panel	Compound	Cells	Phenotypic assay	Unmodified IC_{50} (nM)	Chloroalkane tagged IC_{50} (nM)	Impact (fold)
A	BIRB796*	THP-1	TNFα secretion (ELISA)	8.6×10^{3}	6.5×10^{3}	None
B	Dasatinib	K-562	STAT5 reporter assay Caspase 3/7 assay	3.6×10^{-1} 4.2×10^{0}	1.1×10^{0} 1.8×10^{1}	3.0 4.3
C	SAHA	K-562	HDAC Glo I/II assay Caspase 3/7 assay	1.1×10^{2} 6.6×10^{3}	3.7×10^{2} 2.0×10^{4}	3.4 3.0

Figure 3. Phenotypic outcomes induced by the unmodified compounds (●) and the chloroalkane tagged compounds (○): (A) BIRB796*, (B) dasatinib, and (C) SAHA ($n = 3$). Note the double y-axes in panels B and C indicate different assays. (D) Summary of observed affinities and effect of the chloroalkane tag on the phenotypic outcomes.

primary targets of SAHA, HDACs class I/IIb, differ in their cellular abundance and localization (i.e., nuclear or cytosolic).[26] They also exhibit a range of affinity for SAHA (nM to low μM K_d values) with generally rapid dissociation rates.[25,26,31] Although target engagement by tagged compounds in living cells should provide a more biologically meaningful context, it also presents certain technical challenges, particularly dissociation of transiently bound targets driven by their extensive dilution upon cell lysis. To test the effectiveness of our method relative to enrichment from cell lysates, we optimized both methods for enrichment of HDACs from HEK293T cells (Supporting Information Figure 4). Western analysis indicated that the relatively abundant and high affinity HDAC1 and HDAC2 can be efficiently enriched from either cells or lysates (Figure 4). In contrast, for the less abundant HDAC6 and HDAC3 and lower affinity HDAC8, a significantly higher degree of enrichment was achieved when target engagement occurred inside cells. These results suggest that, at least for this model, engaging the targets within living cells is advantageous, particularly for the enrichment of targets of lower affinity or abundance.

We did not detect any enrichment of HDAC10 and suspected this was due to its significantly low expression levels in HEK293T cells.[32] We repeated the analysis in the phenotypically relevant K-562 cells (used to verify the pharmacology of SAHA-T1) and used more cells in the enrichment experiments. For these samples, Western analysis revealed specific isolation of all the HDACs expected to interact with SAHA, including HDAC10 (Supporting Information Figure 5). Significant enrichment of these HDACs was also apparent by mass spectrometry analysis (LC-MS/MS), demonstrating the effectiveness of this approach

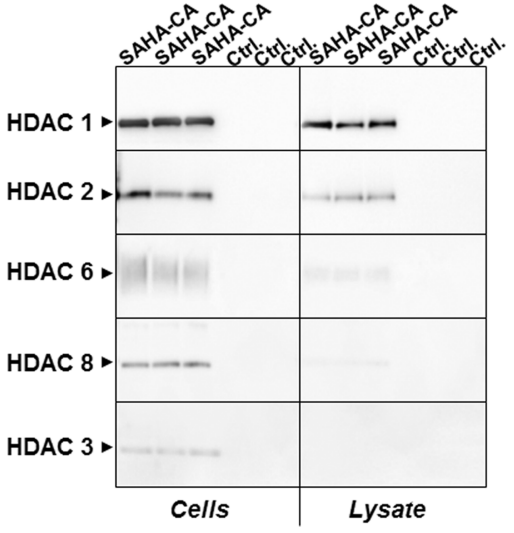

Figure 4. Western analysis of the selective enrichments of SAHA's HDAC targets from HEK293T cells following target engagement in intact cells or in lysate.

to sufficiently preserve the binding interactions throughout the enrichment process. In addition to the expected targets, we also identified two previously undescribed targets, ADO and CPPED1 (Table 1).

Target Verification. From the data presented thus far, we cannot conclude whether the identified proteins bind directly to the compound or are copurified through interactions with direct targets. We have previously shown that BRET can reveal

DOI: 10.1021/acschembio.5b00351
ACS Chem. Biol. 2015, 10, 2316−2324

Table 1. LC-MS/MS Analysis[a]

protein	MW kDa	mean SpC			mean NSAF		
		ctrl.	SAHA-CA	SAHA-CA/ctrl.	ctrl.	SAHA-CA	SAHA-CA/ctrl.
HDAC1	55	28.3	194.3	6.9	1.0×10^{-3}	7.7×10^{-3}	7.3
HDAC2	55	31.3	166.3	5.3	1.2×10^{-3}	6.6×10^{-3}	5.7
HDAC6	131	2.7	235.7	88.4	3.8×10^{-5}	3.9×10^{-3}	102.0
ADO	30	8.7	47.0	5.4	5.9×10^{-4}	3.4×10^{-3}	5.7
HDAC3	49	0	44.0	NA	0	2.0×10^{-3}	NA
CPPED1	36	2.7	24.3	9.1	1.5×10^{-4}	1.4×10^{-3}	9.7
HDAC8	42	1.0	8.0	8.0	5.6×10^{-5}	4.0×10^{-4}	7.2
HDAC10	71	0	6.7	NA	0	2.1×10^{-4}	NA

[a]Proteins specifically enriched from K-562 cells treated with SAHA-chloroalkane. Interacting proteins were determined based on the following criteria: at least five spectral counts in the test sample and none in the control sample or at least 4-fold more spectral counts in the test sample over the control. Data from three different experiments are represented as the mean of spectral counts (SpC) or the mean of normalized spectral abundance factors (NSAF). SAHA-CA= SAHA chloroalkane conjugate, NA = not applicable, fold enrichment can not be determined when the SpC in the control are 0. For results from individual runs and additional details on the LC-MS/MS analysis method, refer to the Supporting Information.

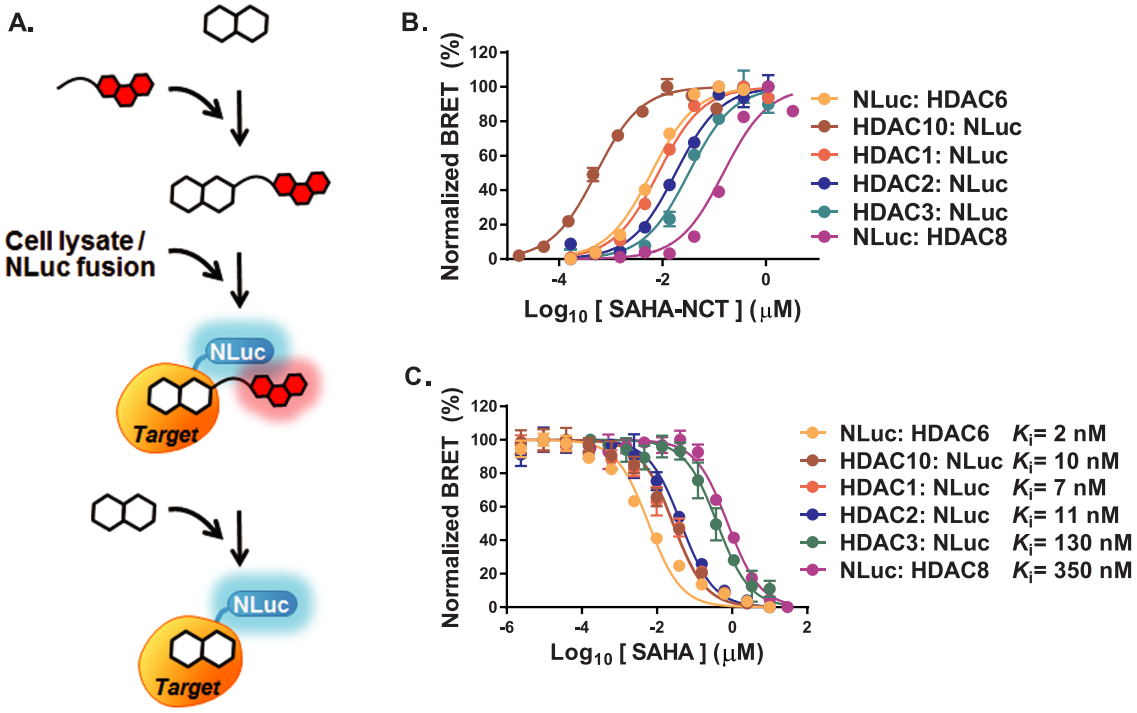

Figure 5. Verification of known HDAC targets of SAHA by BRET: (A) BRET workflow, (B) SAHA-NCT binding (n = 3), and (C) competitive displacement of SAHA-NCT (n = 3). NLuc donor emission wavelength is 460 nm. NCT acceptor fluorophore excitation wavelength is 590 nm, and emission wavelength is 618 nm.

the direct binding relationship of a compound with its protein targets.[24] Because of the rigorous distance constraints imposed by BRET,[22] binding interactions between the fluorophore tagged compound and the luciferase fused to the target can be detected in living cells or lysates without requiring protein purification (Figure 5, panel A).

To determine whether SAHA binds directly to the identified targets, we exchanged the chloroalkane tag with nonchloro-TOM[33] to create SAHA-NCT and generated genetic fusions of NLuc[23] to the eight targets identified by mass spectrometry. By this approach, we confirmed specific, dose-dependent, and saturable binding of the SAHA-NCT to HDACs 1, 2, 3, 6, 8, and 10 (Figure 5, panel B). Apparent affinities for SAHA to these targets were determined by competitive displacement of the SAHA-NCT with unmodified SAHA. Binding constants (K_i) were estimated using the Cheng–Prusoff equation[34] and found to be in general agreement with reported values[25] (Figure 5, panel C). For the two putative novel targets, ADO and CPPED1, we estimated binding constants of 450 nM and 1.2 μM, respectively (Figure 6, panels A and B). CPPED1 (also known as CSPT1) is a serine/threonine phosphatase that specifically dephosphorylates AKT.[35] ADO is a thiol dioxygenase that catalyzes the oxidation of cysteamine to hypotaurine.[36] Neither have been previously reported as a target of SAHA,[12,14,37,38] nor do they exhibit sequence similarities with HDACs. However, both are metalloenzymes capable of binding a divalent transition metal

DOI: 10.1021/acschembio.5b00351
ACS Chem. Biol. 2015, 10, 2316–2324

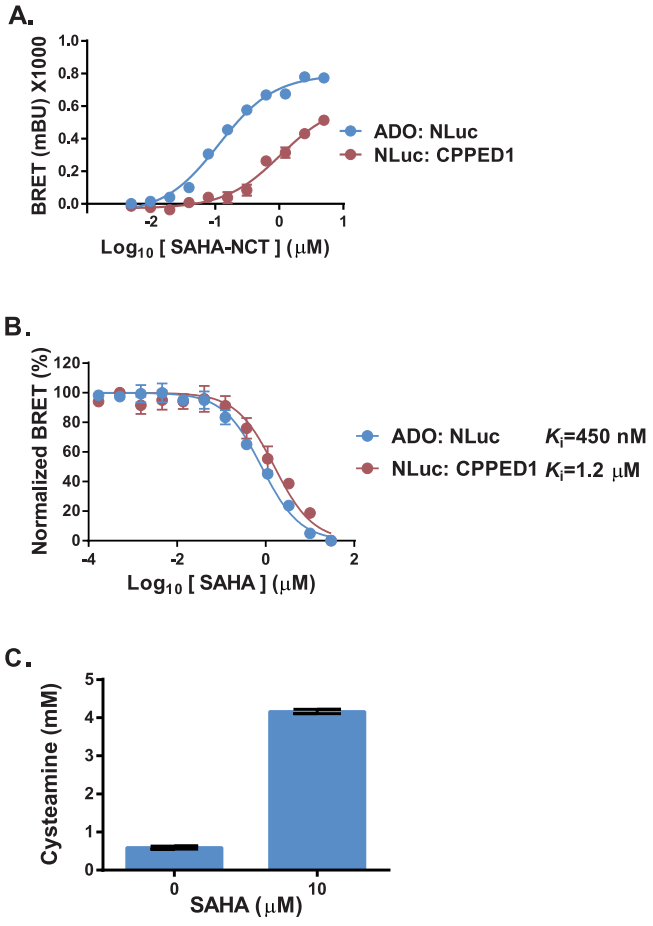

Figure 6. Verification of novel SAHA targets: (A) SAHA-NCT binding (n = 3), (B) competitive displacement of SAHA-NCT (n = 3), and (C) inhibition of ADO activity by SAHA (n = 3).

ion. Since SAHA binds to HDACs, in part by chelating to a bound zinc ion,[25] it may interact in a similar manner with these metalloenzymes.

Our discovery of ADO as a target of SAHA may lend mechanistic insight into the reported efficacy of SAHA in the treatment of Huntington's disease.[27] Cysteamine has been approved as an orphan drug for Huntington's disease, although its rapid metabolism remains a major challenge in sustaining the concentrations necessary for therapeutic effect.[39] It has also been separately reported that cysteamine[40] and SAHA[27] ameliorated the Huntington's phenotype in R6/2 model mice. Both treatments produced similar biological outcomes, improving motor impairment without apparent reduction of neuronal nuclear inclusions, although no underlying mechanism common to these compounds has been proposed. Our results suggest that SAHA may inhibit ADO, thereby increasing the cysteamine levels through suppression of its metabolism. This is further supported by our results indicating that incubation of purified ADO with SAHA inhibited the conversion of cysteamine to hypotaurine (Figure 6, panel C).

Comparison between Chloroalkane and Biotin Tags. As biotin is a commonly used capture tag, we evaluated whether it would be as effective as the chloroalkane tag for the enrichment of SAHA targets. To do this, we exchanged the $(CH_2)_4Cl$ part of SAHA-chloroalkane with an amide-$(CH_2)_4$-biotin, keeping the remainder of T1 intact (Figure 7, panel A). K-562 cells were incubated with both the SAHA-chloroalkane and SAHA-biotin

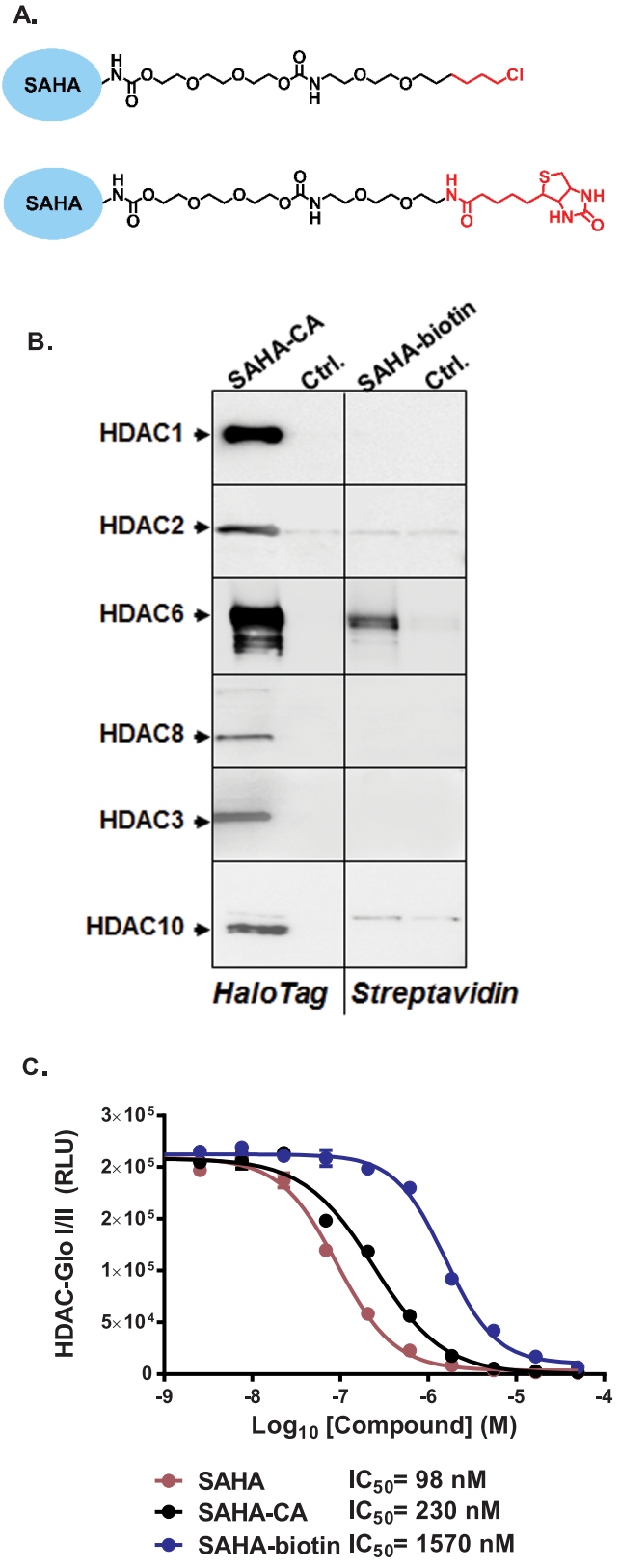

Figure 7. Comparison between chloroalkane and biotin tags: (A) structure of the chloroalkane and biotin tags. The red regions indicate the structural difference between the two tags. (B) Impact of tags on enrichment of SAHA's HDAC targets from K-562 cells analyzed by Western and (C) impact of tags on SAHA potency (n = 3).

DOI: 10.1021/acschembio.5b00351
ACS Chem. Biol. 2015, 10, 2316−2324

to allow intracellular target engagement. Following cell lysis, the SAHA conjugates were captured onto HaloTag or streptavidin paramagnetic particles, respectively, and interacting proteins were released by competitive elution with unmodified SAHA. Western analysis revealed that SAHA-chloroalkane enriched all the expected HDACs, while SAHA-biotin only enriched HDAC6 (Figure 7, panel B).

To examine whether the differential enrichment efficiency was due to an inability of SAHA-biotin to engage the intracellular targets, we tested the potency of both SAHA conjugates in K-562 cells. We found that the chloroalkane tag reduced SAHA potency by 2.3-fold, while the biotin tag reduced it by 16-fold (Figure 7, panel C). The greater impact of the biotin tag may be due to its reported tendency to interfere with compound solubility and cell permeability.[5,10] However, it could also be due to biotin interference with SAHA's cellular interactions. We used the BRET assay to compare the relative affinities of SAHA, SAHA-chloroalkane, and SAHA-biotin to the different HDACs (Supporting Information Figure 7) and found that the biotin tag displayed a higher degree of interference with the SAHA interactions. The effect was most pronounced for the affinities to HDAC 1, 2, and 6, which were reduced only 5- to 6-fold by the chloroalkane tag, but as much as 26- to 65-fold by the biotin tag.

The superior enrichment displayed by SAHA-chloroalkane could be largely the result of a more effective target engagement. However, enhanced capture efficiency by the HaloTag paramagnetic particles may also be a contributing factor. To test this possibility, we compared the SAHA-chloroalkane and SAHA-biotin for their ability to capture purified HDAC6 using HaloTag or streptavidin particles, respectively (Supporting Information Figure 8). The HaloTag particles captured 3.5-fold more HDAC6. Furthermore, the rate of capture was higher by 10-fold. More efficient capture afforded by the HaloTag particles should be of general utility for target enrichment, particularly from living cells, where target isolation is in direct competition with target dissociation from the tagged compound.

Summary. By tethering compounds with a chloroalkane tag, we have developed a new approach for target discovery that relies upon the dynamic binding interactions occurring within living cells. The tag exhibited little effect on pharmacology when appended to a variety of compounds, so we anticipate it will be broadly useful for relating target engagement with phenotypic outcomes. By enabling target engagement within living cells, conditions prerequisite to the desired phenotype can be used for both validating the suitability of tagged compounds to interact with relevant targets and capturing these targets for subsequent identification. Furthermore, using live cells should help maintain cellular nuances required for binding interactions. These features in concert with the verification of the pharmacological activity should increase confidence in the biological relevance of the identified targets.

In the absence of covalent cross-linking, effective enrichment of the targets relies on rapid recovery of the tagged compounds and their interacting targets from cultured cells. This is achieved through rapid binding onto immobilized HaloTag, which competes with the dissociation of interacting targets following cell lysis. For our model compound, SAHA, capture rates displayed by the chloroalkane tag were significantly faster compared to a similarly configured biotin tag, contributing to vastly greater enrichment of HDAC targets. In addition, the high density of chloroalkane-tagged compound covalently captured onto the HaloTag particles creates a high local compound concentration, which should facilitate the retention of bound targets throughout the enrichment process.

The enrichment process by itself cannot specify the relative binding strength of the interactions, or even whether the identified proteins are able to bind with the compound. Our approach also includes a verification method based on BRET, which reveals direct binding relationships with the bioactive compound and provides an estimate of binding affinity. The method is independent of the target enrichment and identification process, and it is not subject to interference from the relative abundance or capture efficiency of the target. Due to the rigorous distance constraints imposed by BRET, direct binding interactions can be quantitatively monitored in a relevant biological context.

Finally, the effectiveness of this new strategy was demonstrated by the identification and verification of all the known SAHA's HDAC targets regardless of their affinity, dissociation rates, abundance, or cellular compartment. The further discovery of certain metalloenzymes as novel targets of SAHA suggests that this new approach may also reveal "off targets" interactions or novel pharmacological pathways.

METHODS

See the Supporting Information for detailed information about materials and methods related to the chemical synthesis of bioactive compound conjugates, synthesis of HaloTag paramagnetic particles, generation of DNA constructs, cell culture, phenotypic assays, mass spectrometry analysis, enzyme activity assays, and analysis of particle capture capacity and kinetics.

Reagents. Detergent lysis buffer: Mammalian lysis buffer (Promega) supplemented with 1:50 dilution of RQ1 DNase (Promega) and 1× RQ1 DNAase buffer. Pull-down buffer: 50 mM HEPES at pH 7.5, 150 mM NaCl, and 0.01% IGEPAL (Sigma).

Analysis of Binding Kinetics to HaloTag Protein. Binding kinetics in cellular lysate: HEK293T cells were transfected in six-well plates with a DNA construct encoding Luc2:HaloTag fusion. Twenty-four hours post-transfection, cells from two wells were collected, harvested, lysed with 1 mL of detergent lysis buffer, and treated with the chloroalkane tagged compound at a final concentration of 1 μM for up to 60 min. After a specified incubation time, an aliquot was removed and treated with HaloTag TMR Ligand (Promega) at a final concentration of 1 μM for 15 min to label the remaining unbound HaloTag fusion protein. The aliquots were resolved on SDS-PAGE and scanned on a Typhoon 9400 fluorescent imager (GE Healthcare). Bands were quantitated using ImageQuant (GE Healthcare), and binding kinetics were determined as the percent binding over time relative to time zero (no chloroalkane tagged compound added). Binding kinetics inside intact cells: HEK293T cells were transfected in 24-well plates with DNA constructs encoding Luc2:HaloTag fusion (ubiquitous expression) or HaloTag:NLS_3 fusion (nuclear expression). Twenty-four hours post transfection, cells were treated with the chloroalkane tagged compound at a final concentration of 10 μM and incubated at 37 °C at 5% CO_2 for up to 120 min. The medium was then replaced with a medium containing 5 μM HaloTag TMR Ligand, and the cells were incubated for an additional 15 min. After the medium was removed, cells were lysed with detergent lysis buffer, and time points were analyzed as described above.

Enrichment of NLuc Fusion Proteins (Target Engagement Inside Cells). HEK293T cells were transfected in a 96-well plate with a DNA construct encoding a NLuc fusion protein (diluted 1:100 with carrier plasmid pCI-neo). Twenty-four hours post-transfection, cells were treated with 20 μM chloroalkane tagged compound, while control cells remained untreated. Following a 2.5 h incubation, the medium was removed; cells were quickly washed with PBS and then lysed with 30 μL/well detergent lysis buffer for 10 min. Cell lysates were diluted 1:2 with pull-down buffer and transferred to a 96-well plate containing 0.5 μL/well settled paramagnetic HaloTag particles. Following 15 min of binding, the unbound fractions were removed. Particles were washed

DOI: 10.1021/acschembio.5b00351
ACS Chem. Biol. 2015, 10, 2316−2324

three times, 3 min each, and the captured NLuc fusions were released by a 15 min competitive elution with 400 μM unconjugated compound. The released NLuc fusions were detected by NanoGlo reagent (Promega) on a GENios pro plate reader (Tecan).

Enrichment of Endogenous Targets. Endogenous targets were enriched from 1×10^7 HEK293T cells/sample or 5×10^7 K-562 cells/sample. The pull-down protocol was performed in triplicate on an HSM 2.0 Heater Shaker Magnet instrument (Promega). Target engagement inside cells: Triplicates were either treated with SAHA-chloroalkane at a final concentration of 20 μM or remained untreated (controls). Following a 2.5 h incubation, the medium was removed. Cells were quickly washed with PBS and then lysed with 2.5 mL of detergent lysis buffer for 10 min. Cell lysates were collected, centrifuged at 3000 × *g* for 1 min, and then the supernatants were diluted 1:2 with pull-down buffer and transferred to 50 mL tubes containing 75 μL of settled paramagnetic HaloTag particles. Following 15 min of binding, the unbound fractions were removed, and particles were washed three times, 3 min each. The particles were then transferred to Eppendorf tubes, and the bound targets were released by competitive elution with 150 μL of 400 μM SAHA (Selleckchem) for 1 h. Enrichment using SAHA-biotin: the same conditions were used for the SAHA-biotin enrichment experiments with the exception of paramagnetic streptavidin particles (GE Healthcare). The streptavidin particles had 2-fold higher binding capacity for a small molecule (i.e biotin); therefore, only 35 μL of settled particles were used for each pull-down sample. Target engagement in lysate: Samples (in triplicates) were washed with PBS and then lysed with 2.5 mL of detergent lysis buffer for 10 min. Cell lysates were collected, centrifuged at 3000 × *g* for 1 min, and the supernatants were diluted 1:2 with pull-down buffer. Triplicates were either treated with SAHA-chloroalkane at a final concentration of 1 μM or remained untreated (controls). Following 2.5 h of binding, the lysates were transferred to 50 mL tubes containing 75 μL settled paramagnetic HaloTag particles, and enrichment was carried out as described above.

Target Verification by BRET. Bulk lysate: HEK293T cells were harvested (200 × *g* for 5 min), resuspended in BRET buffer (50 mM HEPES pH 7.5, 150 mM NaCl) at 5×10^6 cells/mL, lysed by sonication, aliquoted, and stored at −80 °C. Lysates preparation: HEK293T cells were transfected in six-well plates with a DNA construct encoding an NLuc fusion (diluted 1:10 with carrier plasmid pCI-neo). Twenty-four hours post-transfection, cells from each well were collected and lysed with 200 μL of detergent lysis buffer. Lysates were diluted 1:100 into BRET buffer containing a 1:17 dilution of the bulk lysate and dispensed into white 96-well plates. For determining the binding affinity of SAHA-NCT against the targets, serially diluted SAHA-NCT was added to lysates in the presence or absence of 30 μM competing SAHA. Lysates were then equilibrated for 2 h at 37 °C. To measure BRET, Furimazine (Promega) was added at a final concentration of 20 μM, and filtered luminescence was measured on a Varioskan luminometer (Thermo Scientific) equipped with a 450 nm band-pass filter (donor) and a 610-nm long pass filter (acceptor), using 0.5 s integration time. BRET ratios were determined by dividing 610 nm signals by the 450 nm signals. Background-corrected BRET ratios were determined by subtracting the BRET ratios of samples with excess competing SAHA from the BRET ratios in the absence of competing SAHA. Observed EC_{50} and EC_{80} were calculated for each target. For competitive displacement assays, a fixed EC_{80} SAHA-NCT concentration was added to the lysates. Serially diluted SAHA was then added to the lysates and allowed to equilibrate for 2 h prior to BRET measurements (performed as described above). Apparent affinity values for each target were calculated from the observed IC_{50} values according to the Cheng-Prusoff equation.[34]

■ ASSOCIATED CONTENT

Supporting Information

Supporting methods and figures. The Supporting Information is available free of charge on the ACS Publications website at DOI: 10.1021/acschembio.5b00351.

■ AUTHOR INFORMATION

Corresponding Author

*E-mail: rohana@promega.com.

Notes

The authors declare no competing financial interest.

■ ACKNOWLEDGMENTS

We would like to thank M. Wood for modeling the interaction between chloroalkane-T1 and HaloTag.

■ REFERENCES

(1) Gashaw, I., Ellinghaus, P., Sommer, A., and Asadullah, K. (2011) What makes a good drug target? *Drug Discovery Today 16*, 1037−1043.

(2) Swinney, D. C., and Anthony, J. (2011) How were new medicines discovered? *Nat. Rev. Drug Discovery 10*, 507−519.

(3) Bantscheff, M., and Drewes, G. (2012) Chemoproteomic approaches to drug target identification and drug profiling. *Bioorg. Med. Chem. 20*, 1973−1978.

(4) Cisar, J. S., and Cravatt, B. F. (2012) Fully functionalized small-molecule probes for integrated phenotypic screening and target identification. *J. Am. Chem. Soc. 134*, 10385−10388.

(5) Leslie, B. J., and Hergenrother, P. J. (2008) Identification of the cellular targets of bioactive small organic molecules using affinity reagents. *Chem. Soc. Rev. 37*, 1347−1360.

(6) Mackinnon, A. L., and Taunton, J. (2009) Target Identification by Diazirine Photo-Cross-linking and Click Chemistry. *Curr. Protoc. Chem. Biol. 1*, 55−73.

(7) Rix, U., and Superti-Furga, G. (2009) Target profiling of small molecules by chemical proteomics. *Nat. Chem. Biol. 5*, 616−624.

(8) Sleno, L., and Emili, A. (2008) Proteomic methods for drug target discovery. *Curr. Opin. Chem. Biol. 12*, 46−54.

(9) Sato, S., Murata, A., Shirakawa, T., and Uesugi, M. (2010) Biochemical target isolation for novices: affinity-based strategies. *Chem. Biol. 17*, 616−623.

(10) Ziegler, S., Pries, V., Hedberg, C., and Waldmann, H. (2013) Target identification for small bioactive molecules: finding the needle in the haystack. *Angew. Chem., Int. Ed. 52*, 2744−2792.

(11) Bantscheff, M., Scholten, A., and Heck, A. J. (2009) Revealing promiscuous drug-target interactions by chemical proteomics. *Drug Discovery Today 14*, 1021−1029.

(12) Salisbury, C. M., and Cravatt, B. F. (2008) Optimization of activity-based probes for proteomic profiling of histone deacetylase complexes. *J. Am. Chem. Soc. 130*, 2184−2194.

(13) Su, Y., Ge, J., Zhu, B., Zheng, Y. G., Zhu, Q., and Yao, S. Q. (2013) Target identification of biologically active small molecules via in situ methods. *Curr. Opin. Chem. Biol. 17*, 768−775.

(14) Salisbury, C. M., and Cravatt, B. F. (2007) Activity-based probes for proteomic profiling of histone deacetylase complexes. *Proc. Natl. Acad. Sci. U. S. A. 104*, 1171−1176.

(15) Kawamura, A., Hindi, S., Mihai, D. M., James, L., and Aminova, O. (2008) Binding is not enough: flexibility is needed for photocrosslinking of Lck kinase by benzophenone photoligands. *Bioorg. Med. Chem. 16*, 8824−8829.

(16) Sakurai, K., Ozawa, S., Yamada, R., Yasui, T., and Mizuno, S. (2014) Comparison of the reactivity of carbohydrate photoaffinity probes with different photoreactive groups. *ChemBioChem 15*, 1399−1403.

(17) Duckworth, B. P., Xu, J., Taton, T. A., Guo, A., and Distefano, M. D. (2006) Site-specific, covalent attachment of proteins to a solid surface. *Bioconjugate Chem. 17*, 967−974.

(18) Speers, A. E., and Cravatt, B. F. (2004) Profiling enzyme activities in vivo using click chemistry methods. *Chem. Biol. 11*, 535−546.

(19) Encell, L. P., Friedman Ohana, R., Zimmerman, K., Otto, P., Vidugiris, G., Wood, M. G., Los, G. V., McDougall, M. G., Zimprich, C., Karassina, N., Learish, R. D., Hurst, R., Hartnett, J., Wheeler, S., Stecha, P., English, J., Zhao, K., Mendez, J., Benink, H. A., Murphy, N., Daniels, D. L., Slater, M. R., Urh, M., Darzins, A., Klaubert, D. H., Bulleit, R. F.,

DOI: 10.1021/acschembio.5b00351
ACS Chem. Biol. 2015, 10, 2316−2324

and Wood, K. V. (2012) Development of a dehalogenase-based protein fusion tag capable of rapid, selective and covalent attachment to customizable ligands. *Curr. Chem. Genomics 6*, 55−71.
(20) Los, G. V., Encell, L. P., McDougall, M. G., Hartzell, D. D., Karassina, N., Zimprich, C., Wood, M. G., Learish, R., Ohana, R. F., Urh, M., Simpson, D., Mendez, J., Zimmerman, K., Otto, P., Vidugiris, G., Zhu, J., Darzins, A., Klaubert, D. H., Bulleit, R. F., and Wood, K. V. (2008) HaloTag: a novel protein labeling technology for cell imaging and protein analysis. *ACS Chem. Biol. 3*, 373−382.
(21) Martinez Molina, D., Jafari, R., Ignatushchenko, M., Seki, T., Larsson, E. A., Dan, C., Sreekumar, L., Cao, Y., and Nordlund, P. (2013) Monitoring drug target engagement in cells and tissues using the cellular thermal shift assay. *Science 341*, 84−87.
(22) Xu, Y., Piston, D. W., and Johnson, C. H. (1999) A bioluminescence resonance energy transfer (BRET) system: application to interacting circadian clock proteins. *Proc. Natl. Acad. Sci. U. S. A. 96*, 151−156.
(23) Hall, M. P., Unch, J., Binkowski, B. F., Valley, M. P., Butler, B. L., Wood, M. G., Otto, P., Zimmerman, K., Vidugiris, G., Machleidt, T., Robers, M. B., Benink, H. A., Eggers, C. T., Slater, M. R., Meisenheimer, P. L., Klaubert, D. H., Fan, F., Encell, L. P., and Wood, K. V. (2012) Engineered luciferase reporter from a deep sea shrimp utilizing a novel imidazopyrazinone substrate. *ACS Chem. Biol. 7*, 1848−1857.
(24) Stoddart, L. A., Johnstone, E. K. M., Wheal, A. J., Goulding, J., Robers, M. B., Machleidt, T., Wood, K. V., Hill, S. J., and Pfleger, K. D. G. (2015) Application of BRET to monitor ligand binding to GPCRs. *Nat. Methods 12*, 661−663.
(25) Bradner, J. E., West, N., Grachan, M. L., Greenberg, E. F., Haggarty, S. J., Warnow, T., and Mazitschek, R. (2010) Chemical phylogenetics of histone deacetylases. *Nat. Chem. Biol. 6*, 238−243.
(26) Dokmanovic, M., Clarke, C., and Marks, P. A. (2007) Histone deacetylase inhibitors: overview and perspectives. *Mol. Cancer Res. 5*, 981−989.
(27) Hockly, E., Richon, V. M., Woodman, B., Smith, D. L., Zhou, X., Rosa, E., Sathasivam, K., Ghazi-Noori, S., Mahal, A., Lowden, P. A., Steffan, J. S., Marsh, J. L., Thompson, L. M., Lewis, C. M., Marks, P. A., and Bates, G. P. (2003) Suberoylanilide hydroxamic acid, a histone deacetylase inhibitor, ameliorates motor deficits in a mouse model of Huntington's disease. *Proc. Natl. Acad. Sci. U. S. A. 100*, 2041−2046.
(28) Liu, H., Kuhn, C., Feru, F., Jacques, S. L., Deshmukh, G. D., Ye, P., Rennie, G. R., Johnson, T., Kazmirski, S., Low, S., Coli, R., Ding, Y. H., Cheng, A. C., Tecle, H., English, J. M., Stanton, R., and Wu, J. C. (2010) Enhanced selectivity profile of pyrazole-urea based DFG-out p38alpha inhibitors. *Bioorg. Med. Chem. Lett. 20*, 4885−4891.
(29) Rix, U., Hantschel, O., Durnberger, G., Remsing Rix, L. L., Planyavsky, M., Fernbach, N. V., Kaupe, I., Bennett, K. L., Valent, P., Colinge, J., Kocher, T., and Superti-Furga, G. (2007) Chemical proteomic profiles of the BCR-ABL inhibitors imatinib, nilotinib, and dasatinib reveal novel kinase and nonkinase targets. *Blood 110*, 4055−4063.
(30) Gruenbaum, L. M., Schwartz, R., Woska, J. R., Jr., DeLeon, R. P., Peet, G. W., Warren, T. C., Capolino, A., Mara, L., Morelock, M. M., Shrutkowski, A., Jones, J. W., and Pargellis, C. A. (2009) Inhibition of pro-inflammatory cytokine production by the dual p38/JNK2 inhibitor BIRB796 correlates with the inhibition of p38 signaling. *Biochem. Pharmacol. 77*, 422−432.
(31) Lauffer, B. E., Mintzer, R., Fong, R., Mukund, S., Tam, C., Zilberleyb, I., Flicke, B., Ritscher, A., Fedorowicz, G., Vallero, R., Ortwine, D. F., Gunzner, J., Modrusan, Z., Neumann, L., Koth, C. M., Lupardus, P. J., Kaminker, J. S., Heise, C. E., and Steiner, P. (2013) Histone deacetylase (HDAC) inhibitor kinetic rate constants correlate with cellular histone acetylation but not transcription and cell viability. *J. Biol. Chem. 288*, 26926−26943.
(32) Makkonen, K. M., Malinen, M., Ropponen, A., Vaisanen, S., and Carlberg, C. (2009) Cell cycle regulatory effects of retinoic Acid and forskolin are mediated by the cyclin C gene. *J. Mol. Biol. 393*, 261−271.
(33) Machleidt, T., Woodroofe, C. C., Schwinn, M. K., Méndez, J., Robers, M. B., Zimmerman, K., Otto, P., Daniels, D. L., Kirkland, T. A., and Wood, K. V. (2015) NanoBRET − a Novel BRET Platform for the Analysis of Protein-Protein Interactions. *ACS Chem. Biol.*, 150609142923008.
(34) Cheng, Y., and Prusoff, W. H. (1973) Relationship between the inhibition constant (K1) and the concentration of inhibitor which causes 50% inhibition (I50) of an enzymatic reaction. *Biochem. Pharmacol. 22*, 3099−3108.
(35) Zhuo, D. X., Zhang, X. W., Jin, B., Zhang, Z., Xie, B. S., Wu, C. L., Gong, K., and Mao, Z. B. (2013) CSTP1, a novel protein phosphatase, blocks cell cycle, promotes cell apoptosis, and suppresses tumor growth of bladder cancer by directly dephosphorylating Akt at Ser473 site. *PLoS One 8*, e65679.
(36) Dominy, J. E., Jr., Simmons, C. R., Hirschberger, L. L., Hwang, J., Coloso, R. M., and Stipanuk, M. H. (2007) Discovery and characterization of a second mammalian thiol dioxygenase, cysteamine dioxygenase. *J. Biol. Chem. 282*, 25189−25198.
(37) Bantscheff, M., Hopf, C., Savitski, M. M., Dittmann, A., Grandi, P., Michon, A. M., Schlegl, J., Abraham, Y., Becher, I., Bergamini, G., Boesche, M., Delling, M., Dumpelfeld, B., Eberhard, D., Huthmacher, C., Mathieson, T., Poeckel, D., Reader, V., Strunk, K., Sweetman, G., Kruse, U., Neubauer, G., Ramsden, N. G., and Drewes, G. (2011) Chemoproteomics profiling of HDAC inhibitors reveals selective targeting of HDAC complexes. *Nat. Biotechnol. 29*, 255−265.
(38) Fischer, J. J., Michaelis, S., Schrey, A. K., Diehl, A., Graebner, O. Y., Ungewiss, J., Horzowski, S., Glinski, M., Kroll, F., Dreger, M., and Koester, H. (2011) SAHA Capture Compound–a novel tool for the profiling of histone deacetylases and the identification of additional vorinostat binders. *Proteomics 11*, 4096−4104.
(39) Tenneze, L., Daurat, V., Tibi, A., Chaumet-Riffaud, P., and Funck-Brentano, C. (1999) A study of the relative bioavailability of cysteamine hydrochloride, cysteamine bitartrate and phosphocysteamine in healthy adult male volunteers. *Br. J. Clin. Pharmacol. 47*, 49−52.
(40) Karpuj, M. V., Becher, M. W., Springer, J. E., Chabas, D., Youssef, S., Pedotti, R., Mitchell, D., and Steinman, L. (2002) Prolonged survival and decreased abnormal movements in transgenic model of Huntington disease, with administration of the transglutaminase inhibitor cystamine. *Nat. Med. 8*, 143−149.

DOI: 10.1021/acschembio.5b00351
ACS Chem. Biol. 2015, 10, 2316−2324